

Dynamic behavior of the interface of strip-like structures in driven diffusive systems.

Gustavo P. Saracco and Ezequiel V. Albano

Instituto de Investigaciones Físicoquímicas Teóricas y Aplicadas (INIFTA). Facultad de Ciencias Exactas, UNLP, CONICET. Casilla de Correo 16, Sucursal 4, (1900) La Plata, Argentina.

Abstract

In this work, the dynamic behavior of the interfaces in both the standard and random Katz, Lebowitz and Spohn models is investigated via numerical Monte Carlo simulations in two dimensions. These models consider a lattice gas of density $\rho = 1/2$ with nearest-neighbor attractive interactions between particles under the influence of an external driven field applied along one fixed direction in the case of the standard model, and a randomly varying direction in the case of the random model. The systems are also in contact with a reservoir at temperature T . Studying these systems below and at the second-order phase transition critical temperature ($T \leq T_c$), the average interface width W was measured as a function of the lattice sizes and the anisotropic shape factor. It was found that the saturation value W_{sat}^2 only depends on the lattice size parallel to the external field L_y and exhibits two distinct regimes: $W_{sat}^2 \propto \ln L_y$ for low temperatures, which crosses over to $W_{sat}^2 \propto L_y^{\alpha_I}$ near the critical zone, being the roughness exponent $\alpha_I = 1/2$. By using the relationship $\alpha_I = 1/(1 + \Delta)$, the anisotropic exponent of the KLS model was estimated, giving $\Delta = 1$, in agreement to a recently proposed theoretical approach. The low temperature behavior is consistent with a roughening transition at $T = 0$. At the crossover region between both regimes, we observed indications of the bulk critical zone, which corresponds to the second-order phase transition. The time evolution of W at T_c was also monitored and shows two growing stages: first $W \propto \ln t$ for several decades, and in the following times $W \propto t^{\beta_I}$, where β_I is the dynamic exponent of the interface width. From this value we estimated the dynamic critical exponent of the correlation length in the perpendicular direction to the external field, giving $z_{\perp} \approx 4$, consistent with theoretical approaches developed for the standard model. The critical exponents describing the interface behavior of both studied models is the same, strongly suggesting that they belong to the same universality class

PACS numbers: 64.60.Cn; 05.70.Fh; 05.50.+q; 64.60.Ht

1 Introduction

The study of far from-equilibrium systems has attracted increased interest in the last years [1]-[3], mainly due to the lack of theoretical frames, unlike their equilibrium counterparts. However, useful approaches to the understanding of these systems have been developed, like, for example, the analysis of simple models by means of different techniques, such as field theoretical methods, numerical solving of mean-field equations, Monte Carlo simulations, dynamic scaling, etc. By using these procedures it is expected that one can establish and build more general methods to deal

with these systems. Among the simple models studied, we shall focus our attention on the driven diffusive system (DDS) model introduced by Katz, Lebowitz and Spohn (KLS) [4]. The study of the KLS model has attracted growing attention due to its interesting far-from-equilibrium behavior. This interacting lattice gas, driven into nonequilibrium steady states (NESS) by an external field, exhibits remarkable properties such as its non-Hamiltonian nature, the violation of the fluctuation-dissipation theorem, the occurrence of anisotropic critical behavior [1], the existence of a unique relevant length in the anisotropic pattern formation at low temperatures and the consequent self-similarity in the system at different evolution times [5], etc.

The KLS model in two dimensions is defined on the square lattice assuming a rectangular geometry ($L_x \times L_y$) and using periodic boundary conditions. Lattice configurations are defined by means of occupation numbers $n_{i,j}$ for each site of coordinates (i, j) . Assuming nearest-neighbor (NN) attractive interactions between particles of the gas ($J > 0$) and in absence of any driven field, the Hamiltonian (H) of the lattice gas is given by

$$H = -4J \sum_{\langle ij, i'j' \rangle} n_{i,j} n_{i',j'}, \quad (1)$$

where the summation runs over NN sites only. Assuming a driven field E , the coupling to a thermal bath at temperature T is accounted for by a modified Metropolis rate, given by

$$\min[1, \exp(\Delta H - \eta E/k_b T)], \quad (2)$$

where k_b is the Boltzmann constant, ΔH is the change in H after the attempted particle movement and $\eta = [-1, 0, 1]$ is for a particle hopping [against, orthogonally, along] the field. Also, T is reported in units of $J/k_b T$.

It is well known that for high enough temperatures the KLS model exhibits a lattice-gas-like disordered state. However, at low temperatures anisotropic NESS emerge. This ordered phase is characterized by the presence of strips of high particle density crossing the lattice in the direction parallel to the external field. So, for half-density of particles and at a well-defined critical bulk temperature T_c , the KLS model undergoes a second-order phase transition [1]. Extensive Monte Carlo simulations have shown that $T_c \simeq 1.41 T_c^I$, where $T_c^I = 2.269...J/k_b$ is the Onsager critical temperature of the Ising model [1].

The issue of the universality class of the KLS model has become the subject of a long-standing debate. On one hand, several numerical simulations [6] support the universality class predicted by the theoretical field equation of Janssen *et al* [7]. In this case the main nonlinearity is the current term generated by the driven field. On the other hand, Garrido *et al* [8] have revisited the subject from a different approach and found a new Langevin equation, in which the main nonequilibrium effect is due to the underlying anisotropy. This equation was already known because it describes a variant of the KLS model, called random KLS model (RKLS), where the direction of the driven field changes randomly and does not exhibit any driven particle current. According to their results, Garrido *et al* have concluded that the KLS and the RKLS models belong to the same universality class in the limit of infinite driven field. These results have stimulated theoretical discussions [9, 10], and recent numerical results [11, 12] agree with the universality class of the Langevin equation derived from this last approach. However, subsequent numerical simulations [13] may suggest that the KLS model belongs to the class of the Langevin equation early developed by Janssen *et al*.

Besides the bulk phase transition, another interesting feature of the KLS model is the interfacial behavior and the existence of a roughening transition, which consists in the change of the interface

from flat (or smooth) to rough when the temperature increases [14]. Originally studied in crystal growth models, this transition has been theoretically characterized by applying the renormalization group mechanism to a Hamiltonian proportional to the interface surface, plus a periodic potential that mimics the discrete nature of the surface height. It has been found that the transition can be mapped to the Kosterlitz and Thouless type [15] at a nontrivial roughening critical temperature, T_R , where at low temperatures ($T < T_R$), the saturated statistical width W_{sat}^2 (see Section 2) is independent of the linear system size (L) parallel to it. Also, for $T \geq T_R$ one has $W_{sat}^2 \propto \ln L$. The existence of the roughening transition has been confirmed in several simulations of solid-on-solid (SOS) models, measuring observables such as the height-height correlation function, the difference of concentration in the interface layers, the fluctuations in the number of particles belonging to the interface [16], etc., and in experimental work concerning different metallic interfaces [15].

In the Ising model, the existence of a roughening transition at a nontrivial T_R depends on the system dimension. So, for $d = 2$ $T_R = 0$ and for $d = 3$ $T_R \simeq 0.55T_c$ [17]. Here T_c is the critical temperature of the bulk phase transition in the absence of any external field. Furthermore, in the rough phase ($T > T_R$), the structure factor $G(\vec{q})$, defined as the Fourier transform of the height-height correlation function $\langle h(\vec{x})h(0) \rangle - \langle h \rangle^2$, where $h(\vec{x})$ represents the interface height, behaves as $G(\vec{q}) \propto 1/\vec{q}^2$ in the long wavelength limit, where \vec{q} is a $d - 1$ dimensional wave vector of the capillary waves. This leads to a divergence in W_{sat}^2 for spatial dimension $d \leq 3$. In particular $W_{sat}^2 \sim L^p$ for $d = 2$, with $p = 1$.

For the case of the KLS model in $d = 2$, early theoretical studies have shown that the behavior of the interface cannot be treated as independent from the rest of the system, and bulk degrees of freedom must be considered in order to develop a theoretical description [18]. However, this is quite a hard task, so the main results come from the numerical simulations that were focused to study the influence of the external field on the transition, specifically on the exponent p . It has been found that $p \rightarrow 0$ when E increases, indicating the suppression of roughness [19]. Measurements of the height-height correlations have revealed that the singular behavior of $G(\vec{q})$ is less severe than in the Ising model, although these data are affected by finite-size effects and it is not possible to give a more quantitative conclusion [19]. Subsequently, measurements of $G(\vec{q})$ using larger lattices (the lattice size parallel to the interface was up to 600 lattice units) showed a different behavior than in the Ising model ($E = 0$ case). In this case $G(\vec{k}) \propto 1/\vec{q}^{0.67}$ for both $E = 2$ and $E = 50$ [20]. If this behavior persists in the $\vec{q} \rightarrow 0$ limit, it would be consistent with the observed $p = 0$ in the study of the saturation width already commented. It is also important to mention that all the simulations were performed at low temperatures, $T \leq 2.90J/k_b$, in order to keep an interface in the system [20]. Then, new theoretical calculations applied to the KLS model failed to predict a behavior consistent with $p \sim 0$ found in the simulations, mainly due to the presence of the current term in the equation of motion [7]. However, some progress has been made in the RKLS model. It was found that $W_{sat}^2 \propto \ln L$, which is consistent with $p = 0$ [21], and holds above the roughening temperature, namely $T_R = 0$. This behavior was later confirmed through the study of the height-height correlation function by means of the numerical simulations of the model [20].

In view of the outlined controversies and the lack of some conclusive answers to existing open questions, the aim of this paper is to provide an alternative evaluation of the critical exponents that describe the second-order phase transition of the KLS model and to investigate the existence of a roughening transition. In order to achieve this goal, our attention will be focused on the properties of the interface between the high particle density strips and the gas phase, monitoring the behavior of observables such as the interface width, the bulk and interface energies, and their

fluctuations. Our study is based on extensive numerical Monte Carlo simulations of the model and the interpretation of the obtained data by using dynamic scaling theories. We also performed simulations of the RKLS model in order to compare it with the behavior observed for the KLS model. With this study we expect to clarify the controversy about the theoretical frame that describes the bulk critical behavior in the KLS model and, consequently, to establish the universality class of the model.

This paper is organized as follows: in Section 2 the theoretical background is summarized, in Section 3 we give a brief description of the model; in Section 4 we present and discuss our results, and finally in Section 5 our conclusions are stated.

2 Dynamic Scaling Approach for the Interface Roughness of the Strips.

In order to characterize the dynamic evolution of the interfaces in the KLS model, we first measure the *average interface position* (see figure 1), given by

$$\langle h(t) \rangle = \frac{1}{L_y} \sum_{j=1}^{L_y} h(j, t), \quad (3)$$

where $h(j, t)$ is the distance measured from the center of the strip up to the interface at the position of the j -th column at time t , and L_y is the number of columns given by the lattice size in the direction parallel to the interface. Subsequently, the *interface width* or *roughness* is defined as the fluctuations of the interface position

$$W(L_y, t) \equiv \sqrt{\frac{1}{L_y} \sum_{j=1}^{L_y} [h(j, t) - \langle h(t) \rangle]^2}. \quad (4)$$

So, in the simulations we will compute W as a function of time, at different temperatures and using various lattice sizes, in order to study the change of roughness due to the evaporation/condensation of particles at the surfaces of the strip. Of course, due to the selected initial condition, namely a single strip at $T = 0$, the interface has zero width at $t = 0$.

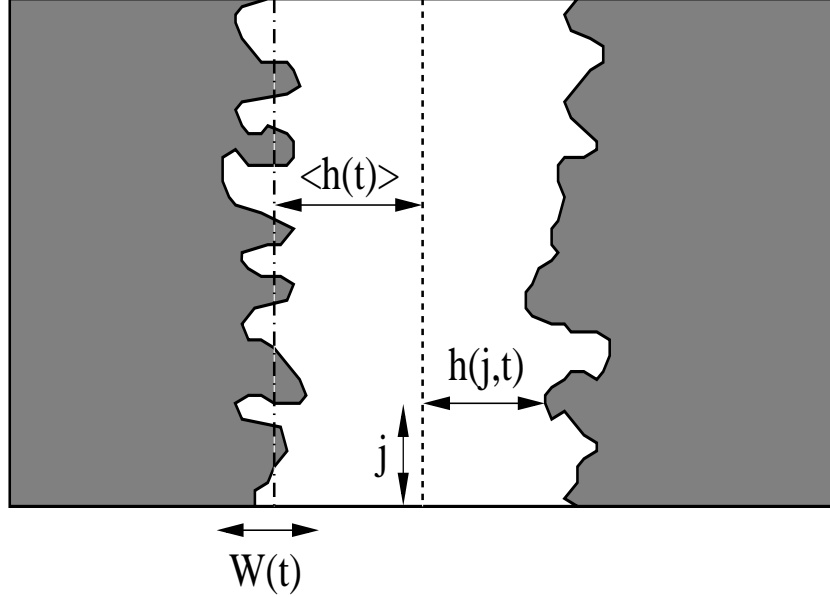


Figure 1: Sketch of a strip of the KLS model (white region) showing the relevant quantities used for the calculations: the distance from the center of the strip (indicated by the dashed line) up to the interface at the position of the j -th column at time t given by $h(j, t)$; the average position of the interface at time t , $\langle h(t) \rangle$ (indicated by the dot-dashed line) (eq. (3)); and the average width of the interface at time t , $W(t)$, given by eq. (4). The gray regions represent the gas phase, and the external field is applied along the vertical axis.

Furthermore, in order to describe the dynamic scaling properties of the interfaces of the strips of the KLS model, we used the scaling Ansatz early proposed by Family and Vicsek [14, 22]. So, it is assumed that the time evolution of roughness obeys the following scaling law

$$W(L_y, t) \sim L_y^{\alpha_I} f\left(\frac{t}{L_y^{z_I}}\right), \quad (5)$$

where $f(u) \propto u^{\beta_I}$ for $u \ll 1$ and $f(u) \rightarrow \text{constant}$ for $u \gg 1$, with $z_I = \alpha_I/\beta_I$. The limit $u \rightarrow 1$ sets the crossover time $t_x \sim L_y^{z_I}$ between both regimes, $u \ll 1$ and $u \gg 1$, respectively. Furthermore, α_I , β_I , and z_I are called the roughness, growth, and dynamic exponents, respectively. We used the subscript “I” in order to distinguish these exponents from those critical exponents of the second-order phase transition of the KLS model.

The dynamic exponent z_I describes the time evolution of the correlation length along the direction parallel to the interface according to $\xi_{\parallel} \propto t^{1/z_I}$ [14]. Thus, for a finite sample of size L and $t \rightarrow \infty$ the correlation length remains finite ($\xi_{\parallel} \simeq L_y$) and the interface width reaches a saturation value that depends on the system size as $W_{\text{sat}}(L_y) \sim L_y^{\alpha_I}$.

In the KLS model, the properties and even the existence of interfaces depend on the temperature T . In fact, for $T \geq T_c$, the system is in the disordered phase and there are no interfaces at all. However, for $T < T_c$, interfaces are present due to the striped patterns characteristic of the ordered

phase (see figure 2). Starting from a single strip placed at the center of the lattice with no holes and two flat interfaces (see Section 3), if the system is annealed to $T > 0$, the particles at the interfaces may leave the strip diffusing into the gas-like phase, causing the width to change (see figure 2). Of course, the inverse process also takes place and some particles of the gas-like phase may stick again at the interfaces, also causing a change in W . Moreover, there are two diffusion processes at the interface: one is driven by the external field, which sets a current along the interface, while the other corresponds to the diffusion of particles in the direction perpendicular to the driving field toward the bulk of the strip.

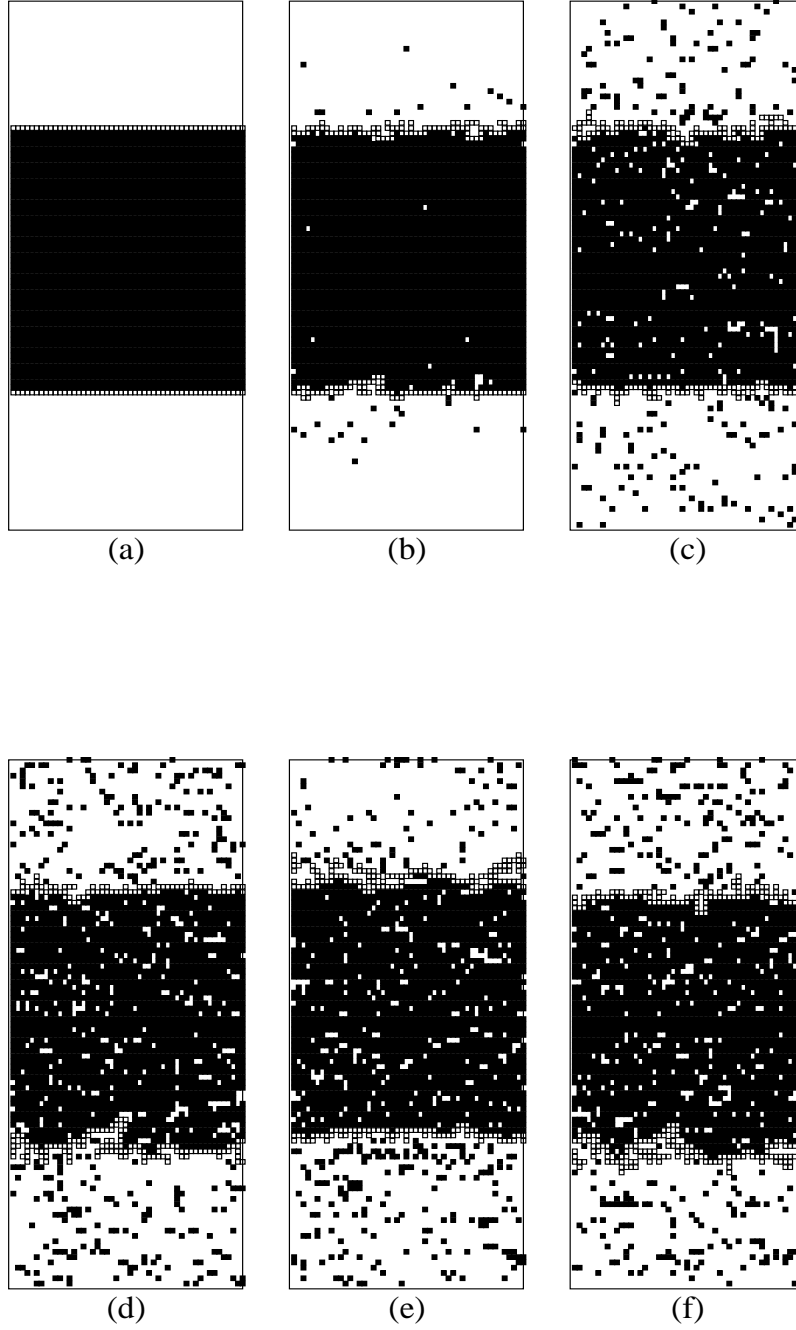


Figure 2: Snapshot configurations corresponding to the IKLS model. Figure (a) shows a single strip containing all particles, corresponding to the ground state configuration ($T = 0$) that is used as initial condition in all simulations reported in this work i.e. at $t=0$. Figures (b)-(f) show the subsequent time evolution of the strip when the system is suddenly annealed to $T = 2.6 < T_c$. The lattice size is $L_x = 100$, $L_y = 50$ (the field direction is the horizontal axis). Particles are shown in black and empty sites are left in white. Empty squares are used to show the interfaces of the strip. From left to right, the corresponding evolution times at which the snapshots were taken are the following: (a) $t = 0$, (b) $t = 100$, (c) $t = 1024$, (d) $t = 10000$, (e) $t = 100480$, and (f) $t = 10^6$.

To adapt the dynamic scaling of Family and Vicsek (eq. (5)) to the KLS model, we have to recall that such system is intrinsically anisotropic and, consequently the exponents entering into equation (5) must be consistent with that anisotropy. As we will see below, the width of the interface saturates for $T < T_c$ due to finite size effects. So, in the limit $u \gg 1$, equation (5) becomes

$$W_{sat}(T) \sim L_y^{\alpha_{eff}} \quad T < T_c, \quad (6)$$

where α_{eff} is the effective (*temperature dependent*) roughness exponent, and L_y is the lattice size along the direction of the external field.

For $T = T_c$, W always diverges with time but, within the time scale used in our simulations (see Section 4), it shows two different growing regimes. Within the first regime W^2 diverges logarithmically, i.e., $W^2 \propto \ln(t)$, and there is also a second regime where W diverges according to a power-law behavior $W \propto t^{\beta_I}$. In this last regime, the correlation length perpendicular to the applied external field (ξ_\perp) is proportional to W and evolves in time according to

$$W \sim \xi_\perp \propto t^{1/z_\perp} \quad T = T_c, \quad (7)$$

where z_\perp is the dynamic exponent of the second-order transition of the KLS model measured along the direction perpendicular to the driving field. Comparing equations (7) and (5) for the limit $u \ll 1$, it follows that $\beta_I = 1/z_\perp$.

The growth of the correlation length in the direction parallel to the applied field (ξ_\parallel) and the fact that the lattice is finite in that direction (L_y) justify the occurrence of a crossover time (t_x) for $T < T_c$. In fact, saturation effects are observed when $\xi_\parallel \sim L_y$ is close to $t = t_x$. Recalling that $\xi_\parallel \propto t^{1/z_\parallel}$ we have that

$$\xi_\parallel(t_x) \sim L_y \propto t_x^{1/z_\parallel}, \quad (8)$$

where z_\parallel is the dynamic exponent of the KLS model along the direction parallel to the applied field. Consequently, from the relation $z_I = \alpha_I/\beta_I$ that holds for the Family-Viscek dynamic Ansatz [22], we have

$$z_I = z_\parallel = \frac{\alpha_I}{\beta_I} = \alpha_I z_\perp, \quad (9)$$

where α_I is the roughness exponent at criticality, i.e., $\alpha_{eff} \rightarrow \alpha_I$ for $T \rightarrow T_c$.

From the scaling theory developed for the KLS model [1], it is well known that the dynamic exponents z_\parallel and z_\perp are related through the anisotropic exponent Δ as follows

$$z_\parallel = z_\perp/(1 + \Delta). \quad (10)$$

Comparing equations (9) and (10) we have

$$\alpha_I = \frac{1}{1 + \Delta}. \quad (11)$$

In this way, by measuring both z_\perp and α_I it would be possible to determine the critical dynamic exponent z_\parallel by using equation (9). Furthermore, one can also compute the anisotropic exponent Δ by using the determined value of α_I . It is worthwhile remarking that $\Delta = 1$ ($\Delta = 2$) has been predicted theoretically by the alternative coarse-grained description of the model developed by Garrido *et al* [8], (by the coarse-grained field theoretical equation developed by Janssen *et al* [7]).

Consequently, the measurement of properties of the interfaces of the KLS model close to criticality is expected to be helpful in order for clarifying the issue of the universality class of the KLS model.

3 Brief Description of the Simulation Method.

The KLS and RKLS models are simulated in a square lattice of size $L_x \times L_y$, where $L_{x(y)}$ is the lattice length in the perpendicular (parallel) direction to the applied drive. Simulations are performed for $62 \leq L_x \leq 208$ and $20 \leq L_y \leq 200$ lattice units (LU), in order to keep the shape factor $S = L_y^{\nu_\perp/\nu_\parallel}/L_x$ fixed and equal to $S = 0.0786$. For setting S we used the critical exponents determined by Garrido *et al* [8], i.e., $\nu_\perp \simeq 0.63$ and $\nu_\parallel \simeq 1.22$. We also performed simulations keeping $L_y = 20$ LU fixed and changing L_x in the range $40 \leq L_x \leq 200$ LU, in order to study the dependence of the interface behavior on L_x . Furthermore, S is not fixed in these lattices, so we can also study the behavior of W_{sat}^2 with the shape factor.

In the case of simulations at the critical temperature, we employed a bigger lattice with $L_x = 524$, $L_y = 346$ LU in order to avoid the early occurrence of finite-size effects.

In all cases the particle density is fixed in $\rho_0 = 1/2$, so that the KLS model exhibits a second-order phase transition [1]. The magnitude of the driving field is kept constant at $E = 50 J$ for all simulations. This value implies, for practical purposes, that we are considering the $E \rightarrow \infty$ limit. So, the studied models become the infinite field KLS model (IKLS) and the infinite random field (IRKLS) model [12]. The temperature is measured in units of J/k_b , k_b being the Boltzmann constant. Under these conditions, the bulk critical temperatures of both models have been estimated in previous work [1, 12, 23], namely $T_c^{IKLS} \simeq 3.20$ and $T_c^{IRKLS} \simeq 3.16$, respectively.

The initial condition from which we started the simulations was the ground state configuration (GSC), which is the configuration that the system has at $T = 0$. It consists of a single strip, free of defects, and placed at the center of the lattice (see figure 2(a)). Subsequently, the time evolution of the interface is followed, measuring its height by identifying the particles belonging to the interface directly, without making any interface coarsening in order to make it a single valued curve [19]. For this we employed the procedure described in ref. [24], which is briefly described in the following way: first of all, we set that particles are connected to their first neighbors (NN), and empty sites are connected to their first and second neighbors (NN and NNN). Then the particle interface can be conveniently characterized by the geographical analogy: the *land* is the set of particles connected to the center of the strip (see figure 1), and the *sea* is the set of connected empty sites not surrounded by the land, otherwise it is called a *lake*. The *islands* are groups of connected particles surrounded by the sea or by a lake. Finally, the *seashore*, which we identify as the *interface*, is the part of the land in contact with the sea. Notice that this description takes into account all particles in the interface, including bubbles and overhangs. Although this is a precise way of identifying the interfaces, we would like to remark that it demands a large amount of CPU time in order to obtain reliable results for each temperature and lattice size.

During a Monte Carlo time step (MCS) each particle in the lattice has an average unitary probability to become selected for an exchange trial. The time evolution of W is monitored until either the strip no longer percolates along the direction parallel to the driving field, or more than one strip is detected.

4 Results and Discussion.

Starting the simulations from the GSC configuration and annealing the system to a temperature $T < T_c$, we monitored the time evolution of the interface roughness. In figures 2(a-f) a typical time evolution of the system from the GSC initial condition is shown. Consequently, the interface width undergoes an initial increase and eventually reaches a saturation value at long enough times. As expected, the saturation value depends on the lattice size, as shown in figure 3 .

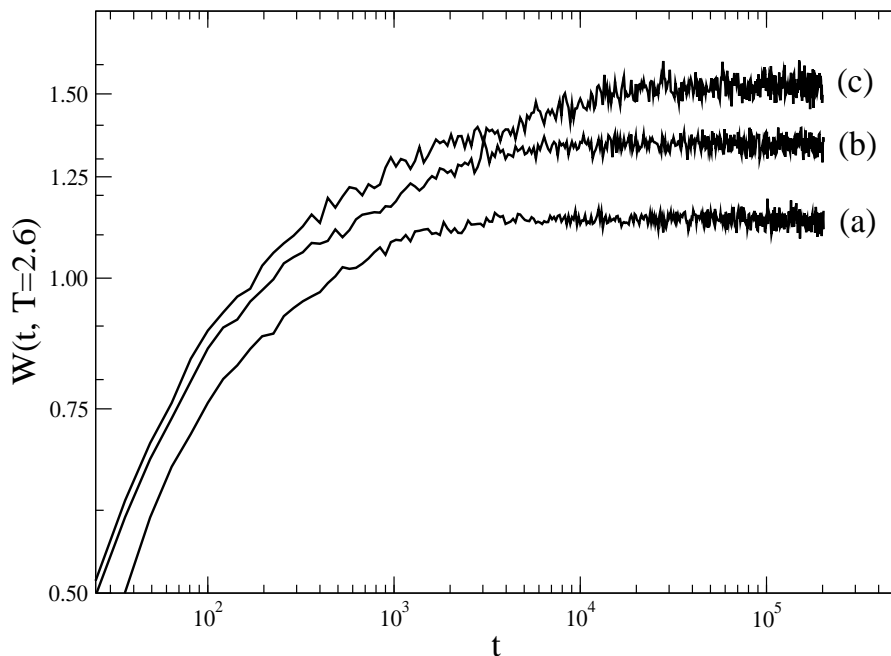


Figure 3: Log-log plots of the interface width W versus t measured at $T = 2.60 < T_c$ for the IKLS model. The lattices used are (a) $L_x = 62$, $L_y = 20$, (b) $L_x = 100$, $L_y = 50$, (c) $L_x = 208$, $L_y = 200$. The curves were obtained averaging over 2000, 300, and 60 different realizations in (a), (b), and (c), respectively.

After determining the saturation value of the interface at different temperatures and using lattices of different sizes, we fitted the data of W_{sat}^2 with the aid of the following Ansatz

$$W_{sat}^2 = A_1 \ln L_y + A_2 L_y^{2\alpha}, \quad (12)$$

where the coefficients A_i 's are temperature dependent and the roughness exponent is taken as $\alpha = 1/2$ (see also below where this assumption is supported by the numerical data). Plots of W_{sat}^2

versus L_y and the corresponding fits obtained by using equation (12) are shown in figure 4.

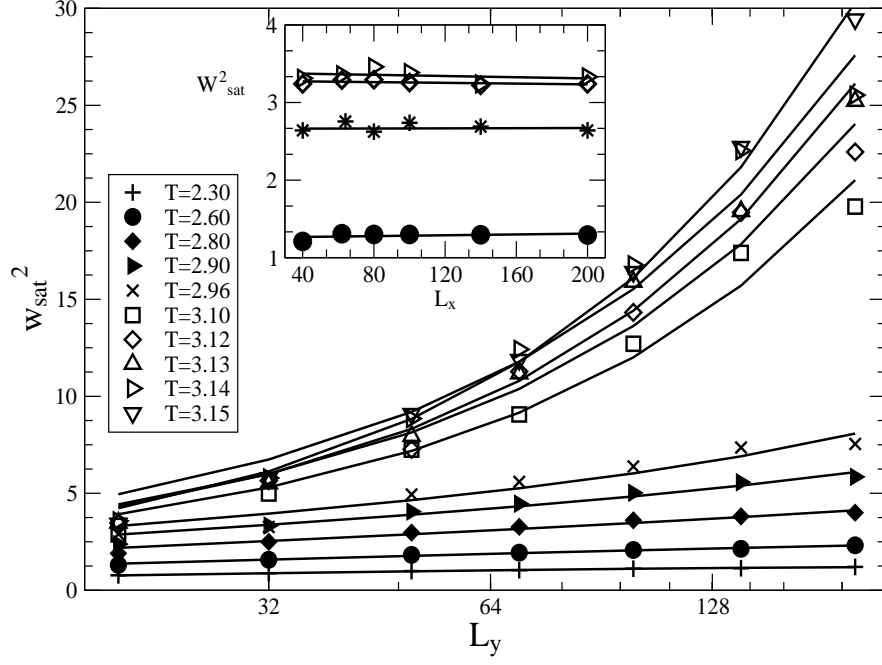


Figure 4: Linear-log plots of the saturation width W_{sat}^2 versus L_y obtained for the listed temperatures. The full lines correspond to regression fits of the measured data by using equation (12). The inset shows the dependence of W_{sat}^2 on L_x and fixed $L_y = 20$, for the temperatures indicated by the legend in the main plot, except $T = 3.00$ indicated by stars. The values of W_{sat}^2 with S fixed are also included in the inset.

Figure 4 shows that the Ansatz (12) fits the saturation values at all temperatures, although the fit is clearly better for lower temperatures, e.g. $T \leq 2.96$. Furthermore, the inset shows that the saturated width does not depend on both the perpendicular lattice size L_x and the shape factor S , since the values of W_{sat}^2 with S fixed are included in the plot, and no difference is noticed from those corresponding to the nonfixed S values. Therefore, we can conclude that our results are not affected by any particular choice of the shape factor.

We also plotted the coefficients A_1 and A_2 versus T , as shown in figure 5, in order to study the temperature dependence of each term in equation (12).

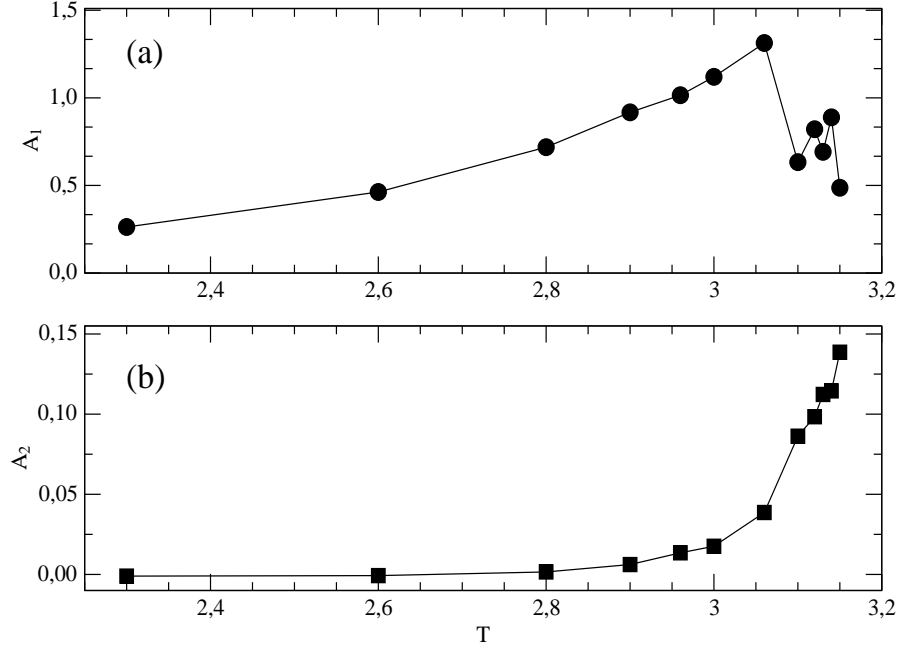


Figure 5: (a) and (b) show linear-linear plots of the coefficients A_1 and A_2 versus the temperature. Data obtained from the fits of the data shown in figure 4 according to eq. (12).

Comparing figures 5 (a) and (b), we can observe that A_2 is almost zero at low temperatures ($T \leq 3.0$) while A_1 increases monotonically. These results indicate that the contribution of the power-law behavior is irrelevant at low temperatures. On the other hand, near the bulk critical temperature ($T \geq 3.0$), A_1 reaches a saturation value around 0.7 and A_2 begins to grow. Although A_1 is about 7 times larger than A_2 , the power-law behavior becomes dominant over the logarithmic one at high temperatures. In view of these results we separately studied both the low and high temperature regimes. In this way, figure 6 shows plots of $W_{sat}^2 \propto \ln L_y$ as obtained within the low T range.

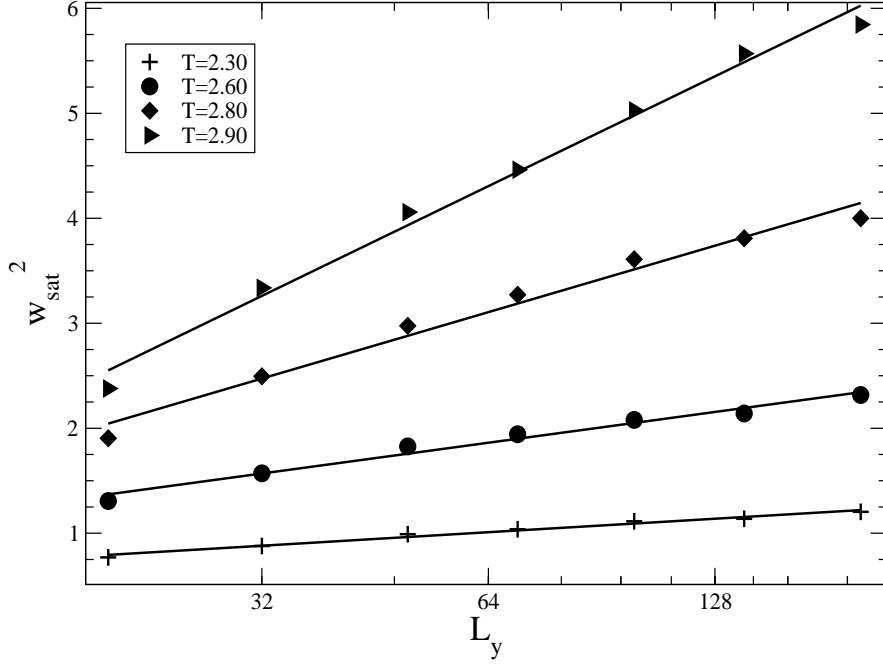


Figure 6: Linear-log plot of the saturation values of the roughness W_{sat}^2 versus L_y , for very low temperatures, as indicated. The data are fitted by the logarithmic term in eq. (12), indicated in the plot by the full lines.

The obtained results showed that the behavior $W^2 \sim \ln L_y$ holds, as it has been predicted theoretically by Zia *et al*, but for the case of the RKLS model [21], and tested numerically in a subsequent work by Leung *et al* [20]. However, to our best knowledge, there are neither theoretical predictions nor numerical tests for the IKLS model that we could use for the sake of comparison. So, this result is consistent with a roughening temperature $T_R = 0$ for the IKLS model such that above T_R the interface width diverges logarithmically.

Within the high-temperature interval, the logarithmic growth crosses over to a power-law behavior (see the power-law term of equation (12)) according to equation (6). Consequently, the effective roughness exponent α_{eff} can be determined for each temperature. Figure 7 shows log-log plots of W_{sat}^2 versus L_y obtained for temperatures close to T_c .

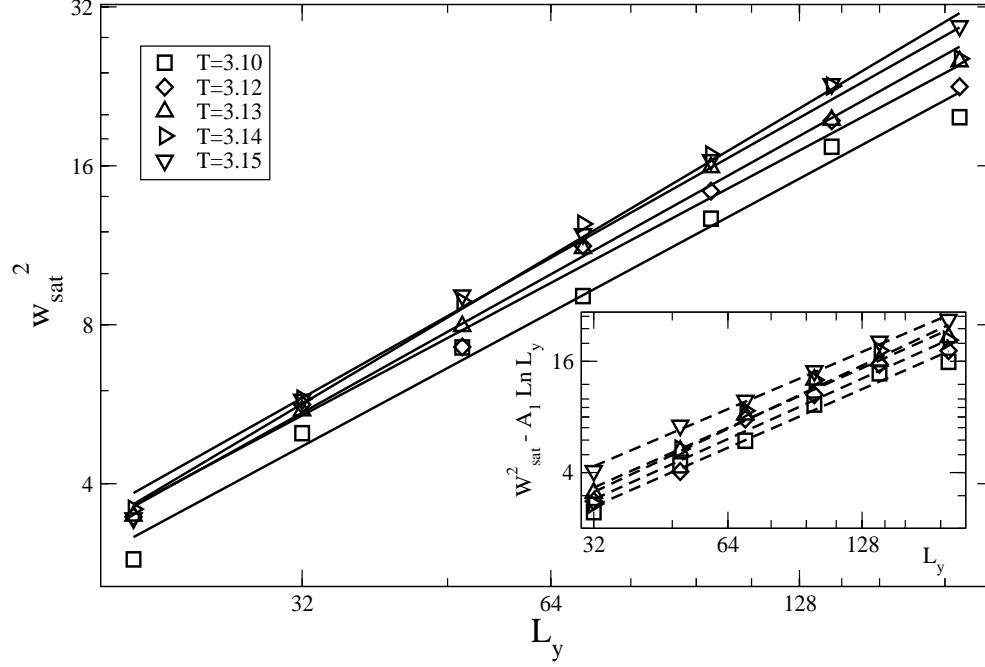


Figure 7: Log-log plots of the saturation width W_{sat}^2 versus L_y evaluated at the indicated temperatures. The inset shows log-log plots of W_{sat}^2 corrected by the logarithmic term in eq. (12) versus L_y . In both plots the data are fitted according to the power-law term expected from eq. (6) and are indicated by full and dashed lines, respectively.

Measuring α_{eff} for different temperatures and plotting the data as a function of the distance to the critical temperature, it is possible to extrapolate the value of α at T_c , as shown in figure 8. According to the trend observed in the plot, it is expected that $\alpha_{eff} \rightarrow 1/2$ for $T \rightarrow T_c$. Actually, a simple linear extrapolation yields $\alpha_{eff}(T = T_c) = 0.477(7)$. However, this value can be improved if we subtract the logarithmic term in equation (12) from the raw data points of W_{sat}^2 . We found that fitting the corrected values with equation (6) (see inset of figure 7), the roughness exponent gives $\alpha_{eff} \approx 1/2$ for all temperatures near T_c , so we can conclude that $\alpha_{eff} \rightarrow 1/2$ in the limit $T \rightarrow T_c$, as predicted by Garrido *et al* [8].

The calculated values of $\alpha_{eff}(T \rightarrow T_c)$ are essential for the clarification of the issue of the universality class of the IKLS model. In fact, using equation (11) it is possible to compute the anisotropic exponent, which gives $\Delta \approx 1$, in agreement with the value predicted by Garrido *et al* on analyzing an alternative mesoscopic equation [8], indicated in figure 8 by the upper dashed line. On the other hand, all determined values of α_{eff} are well above from the estimated value $\alpha = 1/3$, using $\Delta = 2$, as it has been predicted by Janssen *et al* [7] (see the lower dashed line in figure 8).

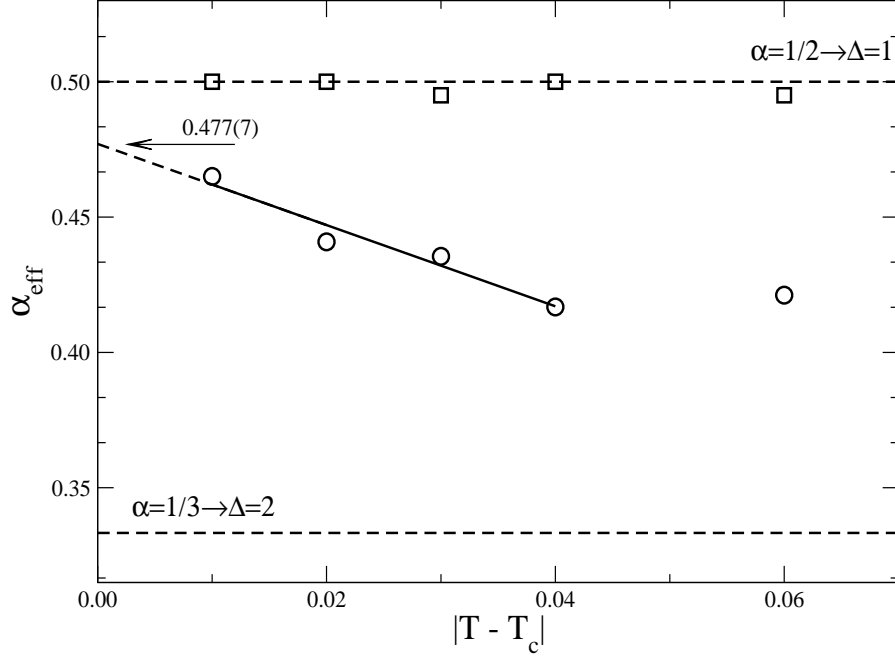


Figure 8: Plot of the effective exponent α_{eff} versus $|T - T_c|$, obtained from the power-law fits of the data shown in figure 7 (open circles), and α_{eff} versus $|T - T_c|$ when W_{sat}^2 is corrected by the logarithmic term in equation (12) (open squares). The dashed lines indicate the theoretical values of α : the upper line is the value obtained by taking $\Delta = 1$, as predicted by the theory proposed by Garrido *et al*, while the lower line shows the value of α obtained by taking $\Delta = 2$, according to the theoretical approach developed by Janssen *et al*. The full line is a linear fit of the data, whose ordinate is $\alpha_{eff}(T = T_c) = 0.477(7)$, as shown by the arrow.

The behavior of W_{sat}^2 around $T \gtrsim 3$ can be investigated in a deeper way by studying the bulk and interface “energies”, given by equation (1), and their fluctuations, defined as

$$\sigma_{B,I} = \langle E_{B,I}^2 \rangle - \langle E_{B,I} \rangle^2. \quad (13)$$

where $E_{B,I}$ is the bulk or interface energy (subscripts B or I , respectively). The obtained results are displayed in figure 9 (a) and (b), respectively.

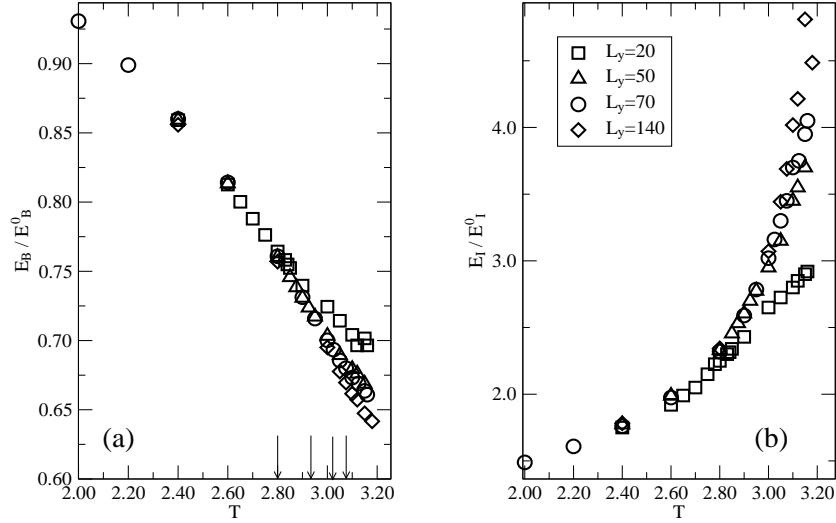


Figure 9: (a) and (b) show plots of the bulk and interface normalized NESS energies corresponding to different sizes L_y (indicated in the legend) versus T . Here E_B^0 and E_I^0 are the energies of the initial GSC configuration. The temperatures where the convexity of figure (a) changes, are indicated by the arrows and increase with increasing L_y .

As the temperature increases, the bulk energy (figure 9 (a)) decreases due to the presence of holes in the bulk and exhibits a small change in the convexity sign for $2.8 \lesssim T \lesssim 3.1$, as indicated by the arrows in the figure. This behavior is similar to that observed in the equilibrium 2d Ising model. On the other hand, the interface energy does not present changes of this kind and grows monotonically due to the interface roughening.

In figure 10 (a) we can observe a peak in the fluctuations of the energy as a function of T for all system sizes parallel to the interface (L_y). However, the interface energy fluctuations grow when both the system size and temperature increase and do not show any peak. These phenomena, together with the (non-) convexity change in the (interface) bulk energy, indicate us that the change in the behavior of W_{sat}^2 with T is in fact a crossover to the bulk critical behavior, and apparently there is no interface phenomena associated with it, such as an extra roughening transition, for example. Consequently, the relationships between the interface exponents α_I , β_I , z_I and the bulk critical exponents are completely justified.

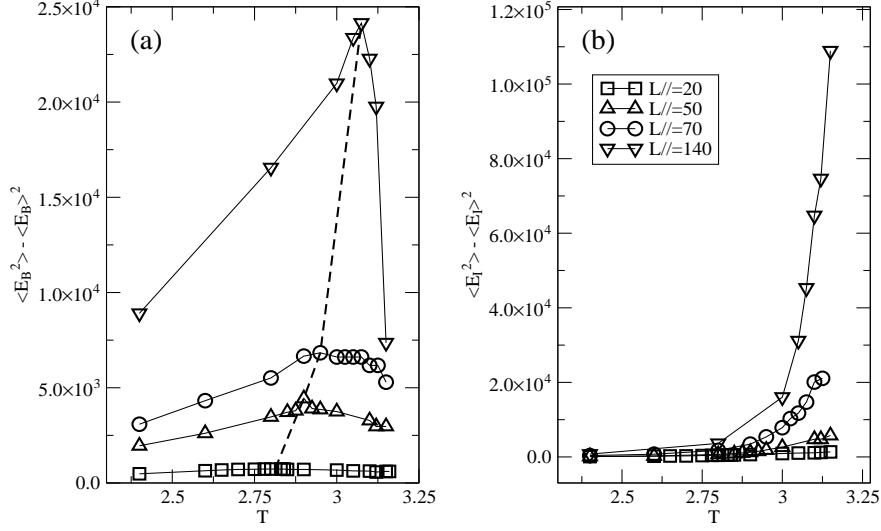


Figure 10: Plots of the bulk energy (a) and interface energy (b) fluctuations. The dashed line in figure (a) indicates the shift of the maxima as a function of L_y .

We have also performed test simulations of the IRKLS model. In fact, figures 11 (a) and (b) show plots of the saturation width versus L_y obtained for three different temperatures and using the same lattice sizes as in the case of the IKLS model. These figures qualitatively show the same behavior already observed for the IKLS model (see figure 4), that is, the saturation width grows logarithmically with L_y at low temperatures, in agreement with the theoretical results of Zia *et al* [21] and the numerical simulations of Leung *et al* [20]. Subsequently, the interface width crosses over to a power-law behavior for $T \lesssim T_c$.

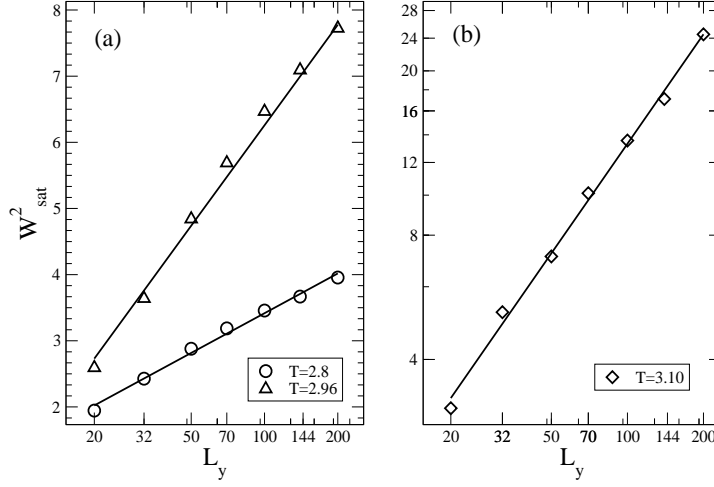


Figure 11: Data corresponding to the IRKLS model obtained at different temperatures, as indicated. (a) Linear-log plots of W_{sat}^2 versus L_y . The full lines are the fit of numerical data with the logarithmic term given by equation (12). (b) Log-log plot of W_{sat}^2 versus L_y . In this case, the numerical data are fitted to a power law of the type $W^2 \propto L_y^{\alpha_{eff}}$, according to eq. (6), or the power-law term in eq. (12).

From the fit in Figure 11, the estimated value of the exponent is $\alpha_{eff}(T = 3.10) = 0.44(2)$, which is compatible with the value estimated for the IKLS model at the same distance to the critical point found in this work. This result is not only in agreement with the fact that $\alpha_I = 1/2$ since we have $\Delta = 1$ in equation (11) for the IKLS model, but also validates our scaling approach for the interface roughness of the IRKLS model.

In order to investigate the critical interfacial properties of both the IKLS and the IRKLS models, we also measured the time dependence of the interface width at T_c , as shown in figure 12. It is worth mentioning that both models exhibit the same behavior at criticality, as evidenced by the (almost perfect) superposition of the numerical results shown in this figure.

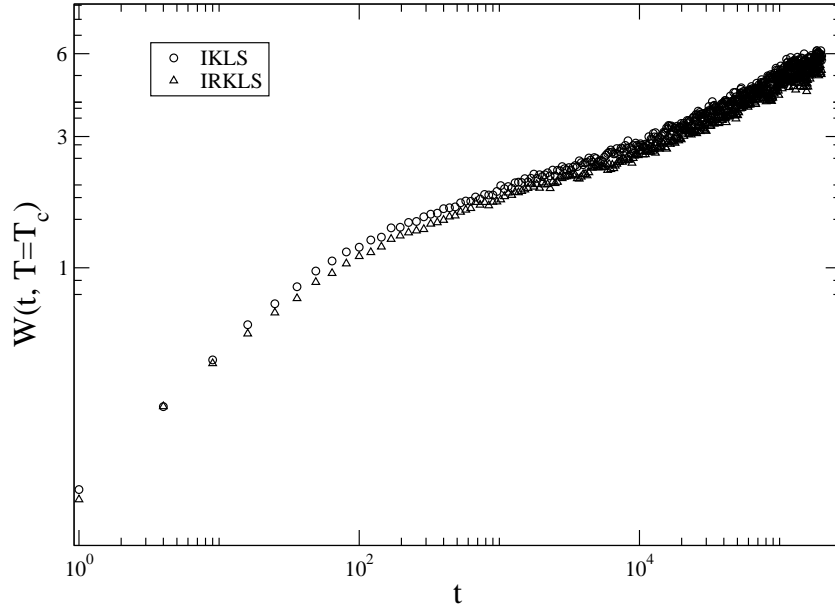


Figure 12: Log-log plots of the interface width W versus t for both the IKLS and IRKLS models, measured at their respective critical temperatures. Results obtained using lattices of size $L_x = 346$ and $L_y = 524$.

Getting further inside the temporal evolution of the width, two well defined growth regimes can be distinguished. At early times the growth is logarithmic $W \propto \ln(t)$, and it lasts almost three decades ($10 - 10^4$ MCS) for both models, see figures 13(a) and 14(a). On the other hand, at a later times, a crossover to a power-law growth regime is observed, that is $W \propto t^{\beta_I}$, as expected from equation (7).

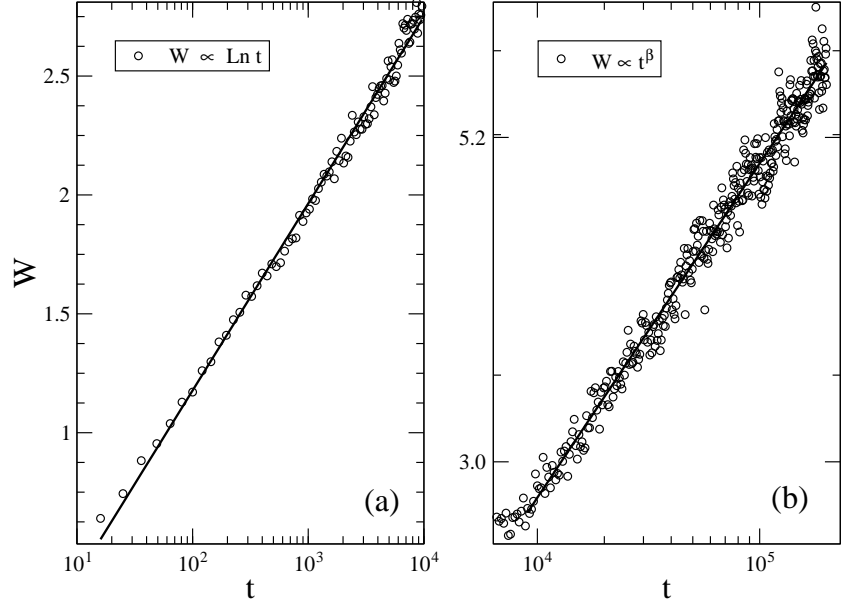


Figure 13: Growth regimes observed during the time evolution of the interface width in the IKLS model at criticality. (a) Logarithmic growth; (b) Power-law growth.

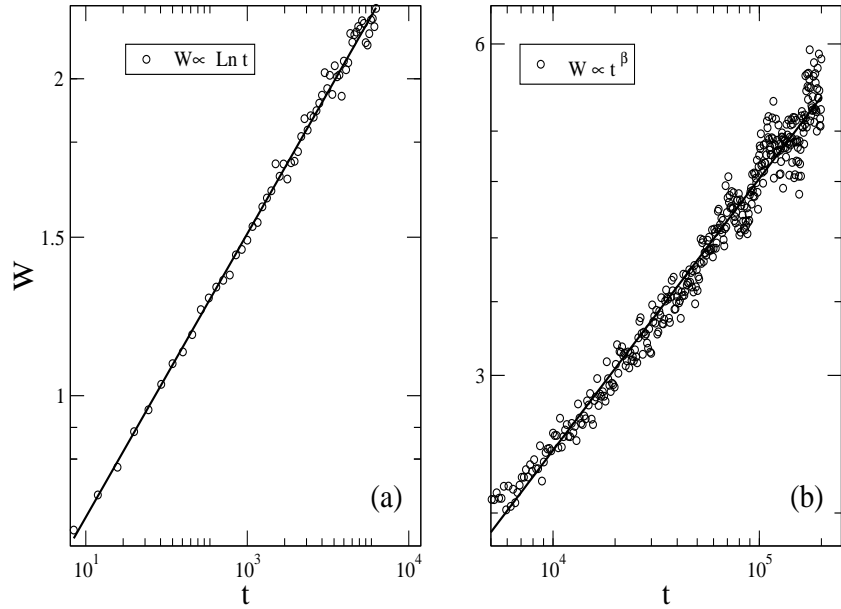


Figure 14: Growth regimes observed during the time evolution of the interface width in the IRKLS model at criticality. (a) Logarithmic growth; (b) Power-law growth.

Focusing on the power-law behavior, we can make a fit of the data to compute the growth exponent of the interface, which yields $\beta_I^{IKLS} = 0.245(2)$, so that $z_{\perp}^{IKLS} = 4.08(4)$ according to equation (7). On the other hand, by fitting the power-law divergence of the interface width for the IRKLS model, the growth exponent $\beta_I^{IRKLS} = 0.247(2)$ is obtained. Therefore, $z_{\perp}^{IRKLS} = 4.05(3)$. As expected, the determination of the dynamic exponent z_{\perp} is not helpful for assigning the universality class of the studied models since, within error bars, theoretical calculations and numerical results are consistent with $z_{\perp} \simeq 4$, for both models and approaches. In any case, these results further validate our scaling approach for the interface roughness in the KLS model.

5 Conclusions.

In this work we studied the dynamic and steady-state behavior of the strip-gas interfaces in both IKLS and IRKLS models. We measured the average width and the roughness exponent α_{eff} for a wide range of temperatures $T \leq T_c$, as a function of the lattice sizes and the shape factor. Starting with the KLS model, the interface width W^2 reaches a saturation value W_{sat}^2 that only depends on the lattice size parallel to the external field direction, L_y . In the low-temperature regime, $T \lesssim 3.0$, W_{sat}^2 exhibits a logarithmic dependence on L_y , as has been theoretically found by Zia *et al* [21] in the RKLS model, and tested numerically in a subsequent work by Leung *et al* [20]. So, our results are consistent with the existence of a roughening temperature $T_R = 0$ for both models such that $W_{sat}^2 \propto \ln L$ for $T > T_R$. Then, close to the critical zone, $3.00 \lesssim T \leq T_c = 3.20$, W_{sat}^2 crosses over to a power law $W_{sat}^2 \propto L_y^{\alpha_{eff}}$. The value of α_{eff} in the limit $T \rightarrow T_c$ was estimated in $\alpha_I = \alpha_{eff}(T \rightarrow T_c) \approx 1/2$. This value is in accordance with $\Delta = 1$, computed by Garrido *et al*, while the predictions of the field-theoretical prediction of Janssen *et al* ($\alpha_I \simeq 1/3$, $\Delta = 2$) can be ruled out.

In order to investigate the change of behavior in W_{sat}^2 around $T = 3.00$, we measured the bulk and interface energies, together with their respective fluctuations. The curves of the bulk energy versus the temperature showed a change in the convexity around the size dependent critical temperature. The fluctuations are peaked at the finite-size critical temperature, and they shift to the infinite-size critical temperature when L_y is increased. In contrast, the interface energy and its fluctuations grow monotonically as the temperature and the lattice size are increased. These facts allow us to conclude that the change in the behavior of W_{sat}^2 around $T = 3.00$ is in fact a crossover to the bulk critical behavior, and apparently it is not related to any interface phenomena such as an extra roughening transition.

Later, the time evolution of the interface width at the critical point was studied. In this case W does not saturate and exhibits two growing stages. In the first stage, W grows logarithmically for several decades, $W \propto \ln t$, and in the following stage W grows obeying a power-law, $W \propto t^{\beta_I}$, with growth exponent $\beta_I = 1/z_{\perp}$. The obtained value of the dynamic exponent was $z_{\perp} = 4.08(4)$, which is in good agreement with the theoretically estimated values, that is $z_{\perp} \approx 3.996$ in Garrido's approach and $z_{\perp} \approx 4$ in Janssen's approach.

On the other hand, the same studies performed on the IRKLS model gave the same results. At low temperatures, $W_{sat}^2 \propto \ln L_y$, confirming the predictions of Zia *et al* [21]. Then, W_{sat}^2 crosses over to a power law at $T \lesssim T_c$, with an effective roughness exponent that is similar to the one measured in the IKLS model at the same temperature. At the critical point, the time evolution of W is the same as in the IKLS model, exhibiting the same logarithmic and power-law growth

regimes. In this last stage the dynamic exponent of the evolution was obtained giving $z_{\perp} = 4.05(3)$, in agreement with that estimated for the IKLS model.

Summing up, our study of the interfacial behavior has proven to be useful for clarifying the issue of the universality class of the IKLS model, so that it can be used as a powerful tool for the characterization of driven diffusive systems.

6 Acknowledgments

This work was made under the support of CONICET, UNLP, and ANPCyT (Argentina). Discussions with M. A. Muñoz are also acknowledged.

References

- [1] B. Schmittmann and R. K. P. Zia, *Statistical Mechanics of Driven Diffusive System*, in Phase transitions and Critical Phenomena, Vol. 17, edited by C. Domb and J. Lebowitz (Academic London, 1995).
- [2] V. Privman (ed.), in: *Nonequilibrium Statistical Mechanics in One Dimension* (Cambridge University Press, 1997)
- [3] J. Marro and R. Dickman, in: *Nonequilibrium Statistical Mechanics Lattice Models* (Cambridge University Press, 1999)
- [4] S. Katz, J. Lebowitz and H. Spohn, Phys. Rev. B **28**, 1655 (1983).
- [5] P. I. Hurtado, J. Marro, P. L. Garrido and E. V. Albano, Phys. Rev. B **67**, 041206 (2003).
- [6] K.-t. Leung, Phys. Rev. Lett. **66**, 453 (1991).
- [7] H. K. Janssen and B. Schmittmann, Z. Phys. B **64**, 503 (1986). K.-t. Leung and J. L. Cardy, J. Stat. Phys. **44**, 567 (1986); ibid **45**, 1087 (1986) (Erratum).
- [8] P. L. Garrido, F. de los Santos and M. A. Muñoz, Phys. Rev. E **57**, 752 (1998). P. L. Garrido, J. Marro, M. A. Muñoz y F. de los Santos, Phys. Rev. E. **61**, R4683 (2000); F. de los Santos, P. L. Garrido and M. A. Muñoz, Physica A **296**, 362 (2001).
- [9] S. Caracciolo, A. Gambassi, M. Gubinelli and A. Pelissetto, Phys. Rev. Lett. **92**, 029601 (2004).
- [10] E. Albano and G. Saracco, Phys. Rev. Lett **92**, 029602 (2004).
- [11] A. Achahbar, P. L. Garrido, J. Marro and M. A. Muñoz, Phys. Rev. Lett. **87**, 195702 (2001).
- [12] E. Albano and G. Saracco, Phys. Rev. Lett. **88**, 145701 (2002).
- [13] S. Caracciolo, A. Gambassi, M. Gubinelli y A. Pelissetto, J. Phys. A: Math. Gen. **36**, L315 (2003); S. Caracciolo, A. Gambassi, M. Gubinelli y A. Pelissetto, J. Stat. Phys. **115**, 281 (2004)
- [14] A. L. Barabási y H. E. Stanley, in *Fractal Concepts in Surface Growth*, Cambridge University Press, New York, 1995.

- [15] J. Lapoujade, Surf, Sci Rep. **20**, 191 (1994).
- [16] J. D. Weeks and G. H. Gilmer, Adv. Chem. Phys **40**, 157 (1979).
- [17] E. Brükner and D. Stauffer, Z. Phys. B **53**, 241, (1983); K. K. Mon, S. Wansleben, D. P. Landau and K. Binder, Phys. Rev. B **39**, 709 (1989).
- [18] K. -t. Leung, J. Stat. Phys. **50**, 405 (1988); C. Yeung J. L. Mozos, A. Hernández- Machado and D. Jasnow, J. Stat. Phys. **70**, 1149 (1993).
- [19] K. -t Leung, K. K. Mon, J. L Vallés and R. K. P. Zia, Phys. Rev. B **39**, 9312 (1989).,
- [20] K. -t. Leung and R. K. P. Zia, J. Phys A: Math. Gen. **26**, L737 (1993).
- [21] R. K. P. Zia and K -t Leung, J. Phys. A: Math. Gen. **24**, L1399 (1991).
- [22] F. Family and T. Vicsek, Phys. A **18**, L75 (1985).
- [23] A. Achahbar, P. L. Garrido, J. Marro, and M. A. Muñoz, Phys. Rev. Lett. **87**, 195702 (2001).
- [24] E. V. Albano and V. C. Chappa, Physica A **327**, 18 (2003).